*Research Journal of Material Sciences* ISSN 2320–6055
Vol. **11(2),** 13-22, August **(2023)** *Res. J. Material Sci.*

# Vacancy formation energy on TiAl alloy in B2 structure at 40, 50 and 60% Al percentages by MEAM method

**Yahnn Jeancy MIGHENSLE MIMBOUI[1,2,4*], Alain Second DZABANA HONGUELET[1,2,4] and Timothée SONGO[1,2,3]**

[1]Faculty of Science and Technology, Marien Ngouabi University, Congo Brazzaville
[2]Research Group on Physical and Chemical Properties of Materials, Congo Brazzaville
[3]Geological and Mining Research Center, Congo Brazzaville
[4]Association Alpha Sciences Beta Technologies, Congo Brazzaville
mimbouiyahnn@gmail.com

**Available online at: www.isca.in, www.isca.me**
Received 11th April 2023, revised 18th June 2023, accepted 23rd July 2023

## Abstract

*In this work, we studied the vacancy formation energy of TiAl alloy of structure B2 of size 10X10X10 for aluminum percentages of 40,50 and 60% under the influence of temperature of 1300, 1400 and 1500°K using the Modified Embedded Atom Method MEAM under the LAMMPS version 2020 calculation code. This study allowed us to understand the behavior of the TiAl alloy under different percentages in terms of total energy, vacancy formation energy, crystal parameter, occupancy rate as well as order parameter. For each of these physical quantities, we have shown that the total energy decreases with temperature, this is also verified for the percentage, the lowest energy is obtained for the structure Ti-60% Al at 1300°K of order-8678.4149meV. For the formation energy, a random behavior is presented to us, caused by the gap, the temperature or the concentration do not predict this behavior, however the structure of Ti-50% Al is well susceptible to form at different temperatures presenting positive formation energies fortemperatures1300, 1400 and 1500°K. The observation on the evolution of the crystalline parameter presents a particular behavior for the alloy Ti-60%Al whose appearance is opposite to that obtained for Ti-40% Al and Ti-50% Al, this reversal occurs around 1350°K, we have assigned this phenomenon to the filling rate. At different temperatures, the occupancy rate remains constant, however the gap does not predict the evolution of the occupancy rate which deviates from the limit value for percentages of 50 and 60%, the largest deviation is obtained for60%Alwhose value is 1.85%. Finally, the order parameter remains positive for the Ti-50% Al structure whatever the study temperature*

**Keywords**: Meam, LAMMPS, Code, Molecular Dynamics, formation energy, order parameter.

## Introduction

For several years, alloys based on the intermetallic compound TiAl have been of growing interest in the scientific community, with a view to structural applications in the aeronautical and automotive sectors. Thanks to their properties, they can also be candidates with high potential and play a key role in military applications (ballistics, armor).

TiAl alloys are intermetallic, with a long-range ordered crystallographic structure. The interatomic bonds are not only metallic, but also covalent, which gives them high strength but also brittleness. The main characteristic of these alloys is to combine a low density (≈ 4g/cm$^3$), about half that of super alloys (≈ 8g/cm$^3$), with high mechanical strength at high temperatures, and good oxidation resistance. These properties give this material great potential in high-temperature industrial, aerospace and automotive applications[1,2].

Antoine PARIS has worked on the study of Phase Transformations in TiAl base alloys with low silicon alloys[3]. The objective of his work was to increase the knowledge related to the precipitation of silicides in titanium aluminides, in order to be able to propose a metallurgical route implementing in an optimized way this structural transformation to, if necessary, improve the mechanical properties of these alloys. To do so, he contributed to develop the knowledge of the phase equilibria in the Ti-Al-Si ternary system. He then characterized the structural modifications of four compositions of alloys, during their solidification and then during solution and precipitation heat treatments.

Sandrine AMELIO led the studies on the micro structural evolution of a TiAl based alloy. Mechanical stress by dynamic compression and thermal stability[4]. This study led to the study of the micro structural evolution of an intermetallic alloy based on TiAl during mechanical solicitations by dynamic compression as well as its behavior during isothermal thermal treatments. The TiAl based alloy studied is characterized by good mechanical properties at high temperature and by a low density.

Professor Timothée NSONGO studied the order-disorder transformation of the TiAl binary alloy system by numerical simulation using the EAM inserted atom method[5]. The aim of this thesis was to determine mainly the influence of the lattice constant, the composition on the type of the order-disorder transformation and the order processes in the alloys.

Mohamed BENHAMIDA has worked on the structural, elastic and electronic properties of transition metal nitride alloys[6]. He studied the structural, electronic and mechanical properties of transition metal nitrides using the DFT density functional theory and compared with experimental results.

The aim of this work was to study the TiAl alloy system in B2 structure at different temperatures (1300, 1400 and 1500 K) according to different atomic percentages of aluminum (40, 50 and 60%) in order to determine the influence of the atomic percentage composition and the temperature on the lattice parameter and to determine its vacation formation energy at these different percentages and temperatures in order to find out at which percentage and temperature the TiAl alloy is stable.

## Methodology

The objective of this study is to provide the vacancy formation energy for different Ti-Al alloys in the BCC phase at operational temperatures. To do so, a 10x10x10 structure of the alloy was simulated, consisting of 2000 atoms in total, in the Large-scale Atomic/Molecular Massively Parallel Simulator (LAMMPS) using a Modified Embedded-Atom Method (MEAM) interatomic potential and a vacancy was created in the middle of the structure. The energy of the structure before and after the creation of the vacancy was used to determine the energy of formation of the vacancy.

In addition to calculating the vacancy formation energy, several different analytical methods were used to determine how vacancy, temperature, and alloying affected the overall cohesion of the atomic structure.

We performed a simulation under the LAMMPS code version 2020 with the executable lmp_mpi, under the Windows operating system, using the MEAM potentials found in the database at https://www.ctcms.nist.gov/potentials/system. The MEAM potentials of Titanium, Aluminium and Ti-Al interaction used in this work were developed respectively by Y.M. Kim, et al.[7], Pascuet and Fernández[8] and Y.K. Kim, et al.[9] are presented in Table-1,2.

These potentials were used to calculate the cohesive energies under different crystallographic structures using the Lammps code and the MPC4 software. The calculations were simulated for periodic crystallographic structures for 10x10x10 mesh under lammps.

**Table-1**: Complementary parameters of titanium and Aluminium.

| Elt | Atwt | Alat | $\beta_0$ | $\beta_1$ | $\beta_2$ | $\beta_3$ | $t_0$ | $t_1$ | $t_2$ | $t_3$ | Esub | Asub | α | Z | Lat | Ibar | Rozero |
|---|---|---|---|---|---|---|---|---|---|---|---|---|---|---|---|---|---|
| Ti | 47.88 | 2.92 | 2.7 | 1.0 | 3.0 | 1.0 | 1.0 | 6.8 | -2.0 | -12.0 | 4.87 | 0.66 | 4.71 | 12 | hcp | 3.0 | 1.0 |
| Al | 26.98 | 4.04 | 3.20 | 2.6 | 6.0 | 2.6 | 1.0 | 3.05 | 0.51 | 7.75 | 3.36 | 1.16 | 4.68 | 12 | fcc | 3.0 | 1.0 |

**Table-2**: MEAM parameters of Ti, Al and Ti-Al

| | Ti | Al | TiAl |
|---|---|---|---|
| Rc (A°) | 4.8 | 4.5 | 4.8 |
| Delr | 0.1 | 0.1 | 0.1 |
| Augt1 | 0 | 0 | 0 |
| Erose_form | 2 | 2 | 2 |
| Ialloy | 2 | 2 | 2 |
| Zbl (1,1) | 0 | 0 | 0 |
| Nn2 (1,1) | 1 | 1 | 1 |
| Rho0 (1) | 1.00 | 1.00 | 1.0 |
| Ec (1,1) | 4.870 | 3.36 | 4.375 |
| Re (1,1) | 2.920 | 2.86 | 2.80 |
| Alpha (1,1) | 4.71945 | 4.68 | 5.562 |
| Repuls (1,1) | 0.00 | 0.05 | 0.0250 |
| Attract (1,1) | 0.00 | 0.05 | 0.0250 |
| Cmin (1,1,1) | 1.00 | 0.49 | 0.4900 |
| Cmax (1,1,1) | 1.44 | 2.80 | 1.4400 |

Here is the crystal structure of the Ti Alalloy in B2 structure.

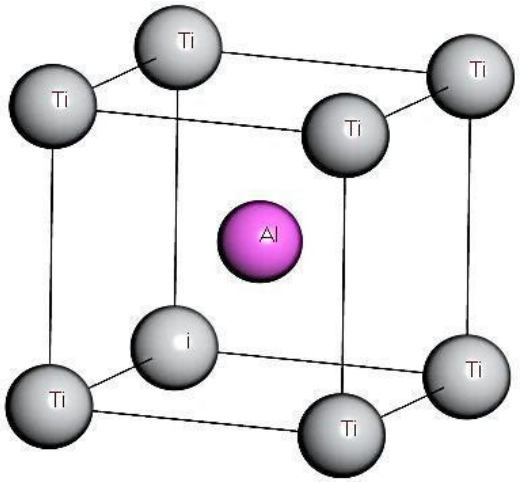


**Figure-1:** Crystalline structure of TiAl in B2 (CsCl).

**Molecular dynamics:** Molecular dynamics computational methods use an interatomic potential to correctly simulate how atoms in a structure interact with each other. In this case, the Modified Embedded-Atom Method (MEAM) was used.

The molecular dynamics code used in this research is LAMMPS (Large-scale Atomic/Molecular Massively Parallel Simulator). The initial setup consisted of 2000 atoms with periodic boundary conditions in a perfect, unrelaxed BCC lattice. The atoms were then allowed to relax by running them in an isothermal -isobaric (NPT), where the number of atoms, pressure and temperature are kept constant. Then, the central atom is removed and the remaining 1999 atoms are run in a canonical set (NVT), where the number of atoms, volume and temperature remain constant.

**Alloy:** Several alloys with different atomic percentages are used here: titanium alloys with 40%, 50% and 60% aluminum. In real life, alloys never have exactly the right atomic percentage. In order to simulate this phenomenon correctly, the atoms have been changed randomly. Starting with a 10x10x10 Ti-Al BCC structure, each atom had a chance to become titanium, this chance being the atomic percentage of aluminum desired in the structure.

**Vacancy formation energy:** In order to calculate the energy of formation of a vacancy, a single vacancy was introduced in a perfect lattice with equilibrium lattice constants and structural relaxation of atomic positions. Only isolated defects without interaction were considered when calculating the defect formation energy[10,11].

In general, the energy of formation of a vacancy in a homogeneous bulk crystal that does not change phase can be described by:

$$Ev=(n\text{-}1)\text{-}[n\text{-}1/n]En \quad (1)$$

E(n-1) is the total energy of an atomic supercell containing a vacancy, while En is the total energy of that supercell before the vacancy was created. In this research, the energy of vacancy formation was calculated by taking averages in three different ways illustrated in the results section.

**Short range order parameter:** The order parameters allow to quantify the configuration and order of a structure in simple and easy to understand values without even looking at the structure itself. The Short-Range Order (SRO) parameter uses only the first nearest neighbors of the atoms to give a single number to represent the order of the structure[12].

$$\sigma = -\frac{P_{AA}-n_A}{1-n_A} \quad (2)$$

## Results and discussion

We present in this part the results obtained on the total energy before and after the creation of the vacancy, the crystalline parameter under the effect of temperature, the occupancy rate as well as the order parameter at short range all these physical quantities under the effect of operational temperatures 1300, 1400 and 1500K.

**Total Energy and Vacancy Formation Energy:** As discussed in the methods section, the vacancy formation energy was calculated using three different methods; the first and third methods used the total energy of the atomic structure, while the second method used the energy per atom by dividing the total energy by the number of atoms currently in the lattice[13].

As a result, the first and third methods provide incredibly similar results, which are also of the same order of magnitude as the previous literature on the vacancy formation energy of titanium.

The results reported on total energy before and after vacancy creation are presented in Table-3, 4.

**Total energies:** We present here the results of methods 1 and 2 on the total energy in Table-3,4. We noticed that the total energy increased with the temperature and decreased with the percentage of aluminum whatever the method used.

**Table-3:** Initial energy method 1.

| Temperature (K) | Total energy | | |
|---|---|---|---|
| | % Al | | |
| | 40 | 50 | 60 |
| 1300 | -8170.05 | -8436.89 | -8678.41 |
| 1400 | -8142.67 | -8428.43 | -8656.42 |
| 1500 | -8136.42 | -8418.12 | -8645.96 |

The initial energies follow the same order regardless of the temperature or the percentage of aluminum in the T-Al alloy.

**Table-4:** Total initial and final energy method 2.

| Temperature (K) | Total initial and final energy | | |
|---|---|---|---|
| | % Al | | |
| | 40 | 50 | 60 |
| 1300 | -8168.10 | -8437.57 | -8674.56 |
| | -8162.57 | -8431.35 | -8673.85 |
| 1400 | -8149.40 | -8425.44 | -8662.03 |
| | -8148.37 | -8419.08 | -8661.30 |
| 1500 | -8140.42 | -8412.69 | -8642.52 |
| | -8134.64 | -8406.88 | -8641.29 |

The final energies obtained after creation of the vacancy also follow the same order of magnitude as the initial energies whatever the operating temperature and or the percentage of aluminum in the Ti-Al alloy. For reliability reasons, these results show a discrepancy with the other two methods 1 and 3; these results just allowed us to confirm that the gap does not influence the total energy of a structure.

**Energy of formation:** These results here of the third method are consistent with the results of the first method, are grouped in Table-3. The values of the formation energy obtained interpret the possibility of obtaining the structure at any temperature.

For 40% Al: the structure can be formed around 1300°K beyond which it becomes very unstable with negative formation energies for 1400 and 12500°K;
For 50% Al: the structure is well stable whatever the operational temperature, this is reflected by the positive formation energies;
For 60% Al: the structure presents a stability beyond 1400°K. The total energy is of no significance to the energy of formation of the vacancy.

These results from methods 1, 2 and 3 reveal that as the temperature increases, the more the structure tends to be more stable as the percentage of aluminum increases.

**Table-5:** Formation energy (method 3).

| Temperature (K) | Formation energy (Method 3) | | | | | | | | |
|---|---|---|---|---|---|---|---|---|---|
| | % Al | | | | | | | | |
| | 40 | | | 50 | | | 60 | | |
| Energy | Ei | Ef | Ef | Ei | Ef | Ef | Ei | Ef | Ef |
| 1300 | -8170.05 | -8158.83 | 7.13 | -8436.89 | -8423.84 | 8.82 | -8678.41 | -8674.96 | -0.88 |
| 1400 | -8142.67 | -8150.23 | -11.63 | -8428.43 | -8420.68 | 3.54 | -8656.42 | -8665.58 | -13.48 |
| 1500 | -8136.42 | -8138.33 | -5.97 | -8418.12 | -8405.97 | 7.93 | -8645.96 | -8640.05 | 1.57 |

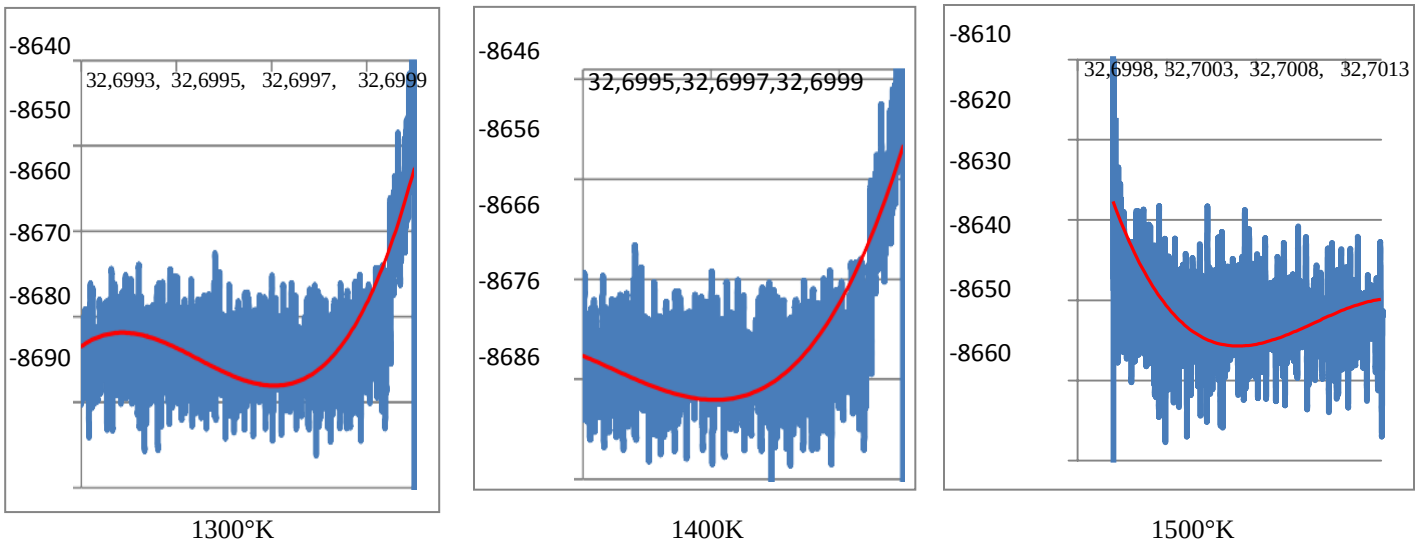


1300°K 1400K 1500°K

**Figure-2:** Polynomial trend energy vs crystal parameter for 60% Al.

**Formation energy:** The behavior observed on the energy of formation caused by the vacancy revealed by the Table-3, is almost random for different temperatures but presents an evolution in "V", for the same concentration whose order is translated by high-low-medium energy of formation such as we have represented it by the Figure-2.

This Figure-1, shows us that whatever the temperature the Ti-50% Al structure remains possible contrary to the two others of 40% Al and 60% Al which present stability at the lower and higher extremes respectively. However, above 1400°K the 60% Al structure is more stable than the 40% Al one. Around 1450°K, Ti-40% Al and Ti-60% Al would present the same mechanical properties.

**Influence of the temperature on the mesh parameter:** We have followed the behavior of the mesh parameter for each of these titanium alloys, the results are presented in Table-4. The variation of the crystalline parameter was of capital interest.

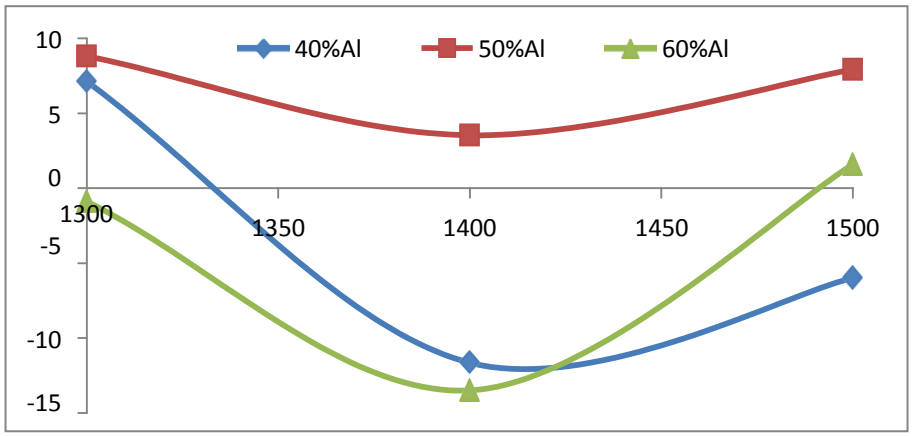


**Figure-2:** Formation energy method[3].

**Table-6:** Mesh parameter evolution by temperature and % Al.

| Temperature (K) | Temperature and lattice parameter | | | | | | | | |
|---|---|---|---|---|---|---|---|---|---|
| | % Al | | | | | | | | |
| | 40 | | | 50 | | | 60 | | |
| | Init | Final | Diff | Init | Final | Diff | Init | Final | Diff |
| 1300 | 32.7 | 32.695282 | 0,004718 | 32.7 | 32.69687 | 0,00313 | 32.7 | 32,699202 | 0,000798 |
| 1400 | 32.7 | 32.696764 | 0,003236 | 32.7 | 32,69838 | 0,00162 | 32.7 | 32,700829 | 0,000829 |
| 1500 | 32.7 | 32.698274 | 0,001726 | 32.7 | 32.699534 | 0,000466 | 32.7 | 32.702053 | 0,002053 |

**Table-6:** Mesh parameter evolution by temperature and % Al

| Temperature (K) | Temperature and lattice parameter | | | | | | | | |
|---|---|---|---|---|---|---|---|---|---|
| | % Al | | | | | | | | |
| | 40 | | | 50 | | | 60 | | |
| | Init | Final | Diff | Init | Final | Diff | Init | Final | Diff |
| 1300 | 32.7 | 32.695282 | 0,004718 | 32.7 | 32.69687 | 0,00313 | 32.7 | 32,699202 | 0,000798 |
| 1400 | 32.7 | 32.696764 | 0,003236 | 32.7 | 32,69838 | 0,00162 | 32.7 | 32,700829 | 0,000829 |
| 1500 | 32.7 | 32.698274 | 0,001726 | 32.7 | 32.699534 | 0,000466 | 32.7 | 32.702053 | 0,002053 |

For 40% Al: we observe a considerable evolution of the crystalline parameter translated by the difference between initial and final crystalline parameter; we note that the more the temperature increases the less the structure is deformed.
For 50% Al: although the difference decreases with temperature, it decreases negligibly proving that the structure is stable around 50% Al;
For 60% Al: this structure presents a contrary tendency to the 40% and 50% Al structures.

A particular phenomenon is reported and which is interpreted by the growth of the mesh parameter, this is observed around 1450°K. We cannot however affirm that this phenomenon is consequent to the presence of the lacuna in the 60% Al structure.

Figures-3 and 4 show us that at equal temperatures, the structure, the difference of the crystalline parameter decreases with the percentage, the more the percentage is considerably less the structure is deformed.

**Crystalline parameter:** We have represented the curve of the crystalline parameter as a function of the pitch to analyze the behavior of the structure. It was observed that the final structures do not have the same parameters (reveals Table-4).

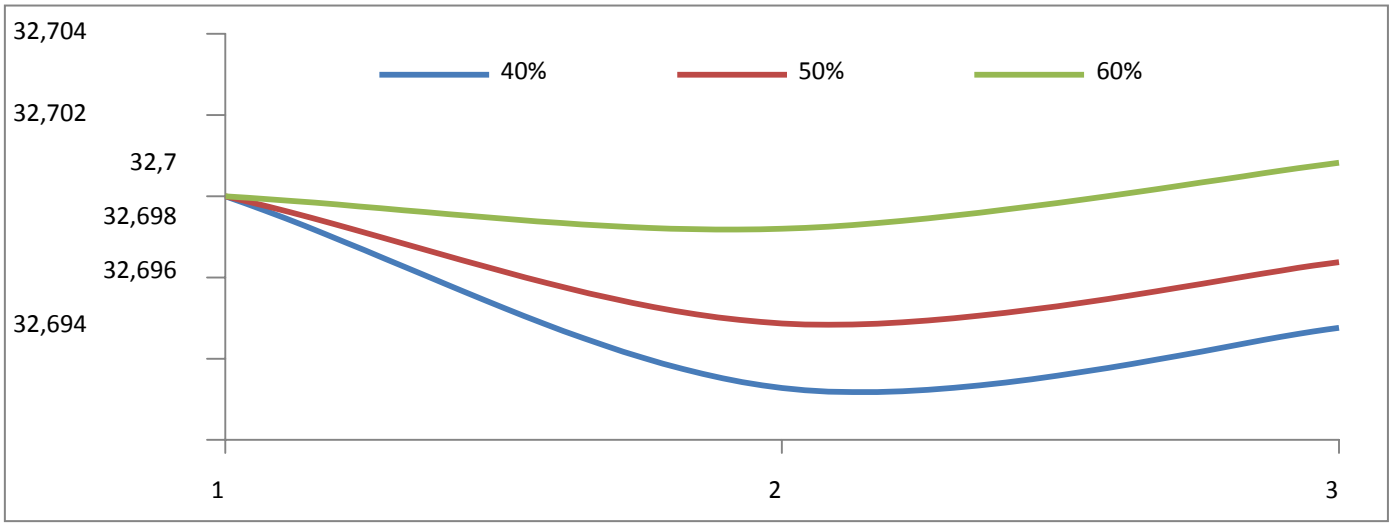


**Figure-3:** Mesh parameter by Temperature.

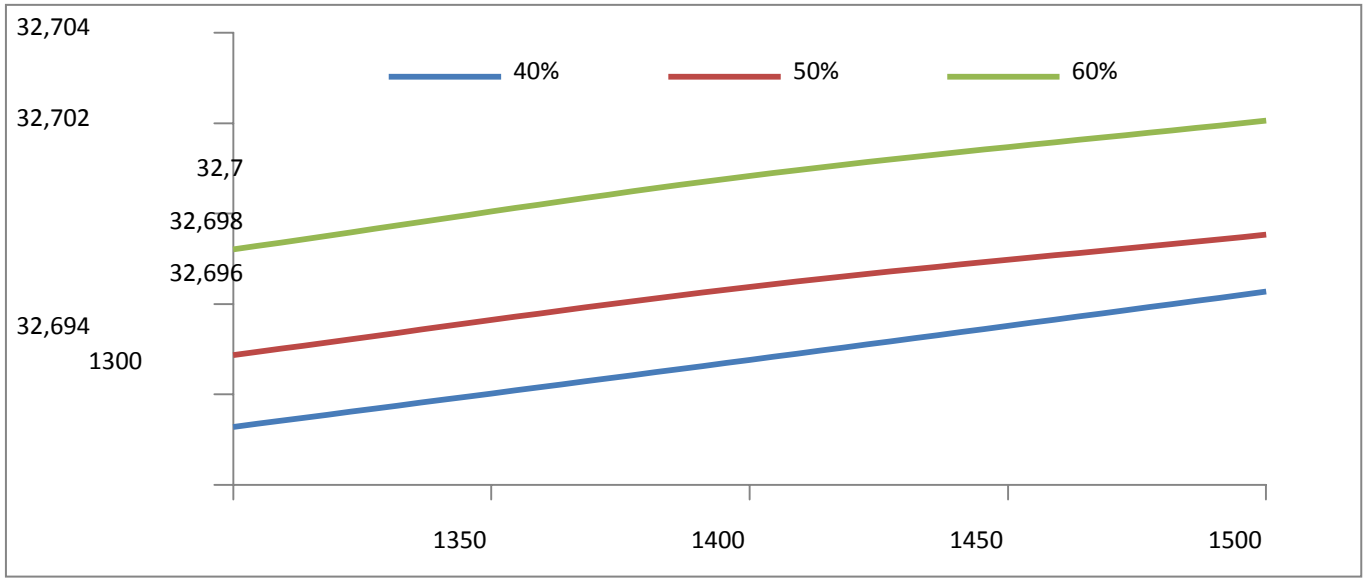


**Figure-4:** Mesh parameter by % Al.

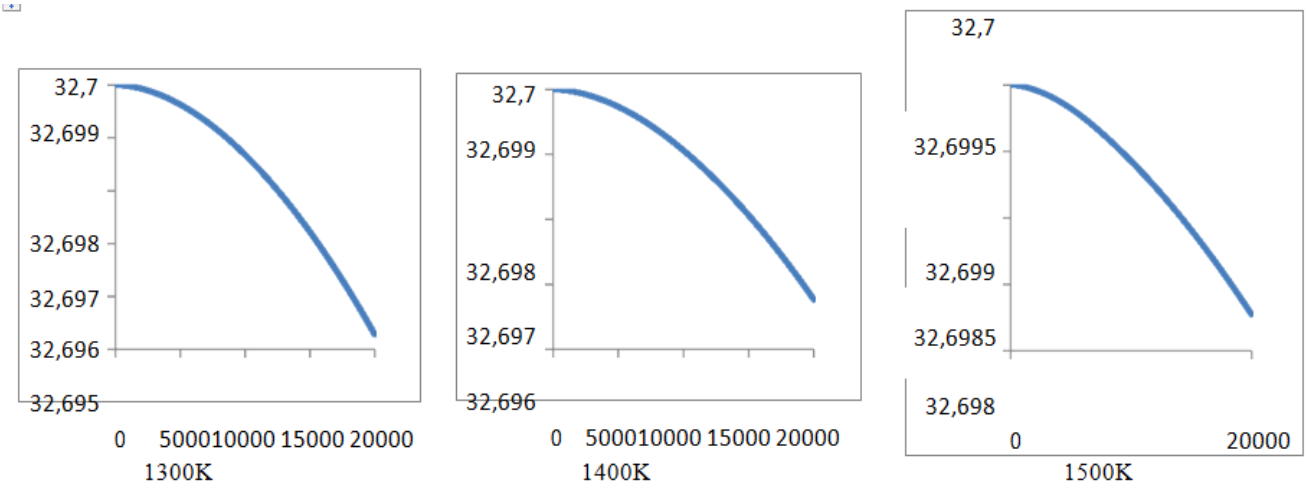


**Figure-5:** parameter plot for 40%Al. For 40% Al: the speed is identical, whatever the temperature.

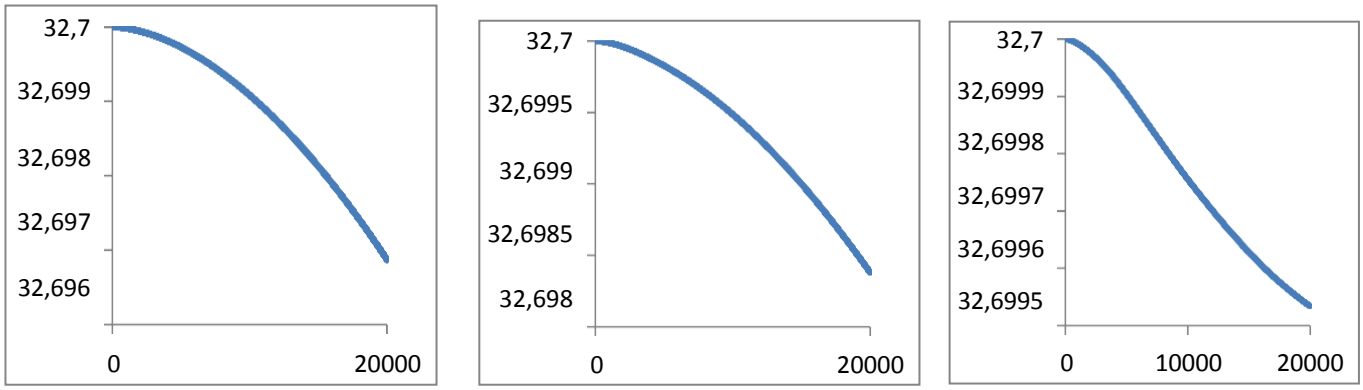


**Figure-6**: Parameter plot for 50% Al. For 50% Al: the trend is identical for operating temperatures below 1500°K, temperature at which the evolution of the parameter becomes linear.

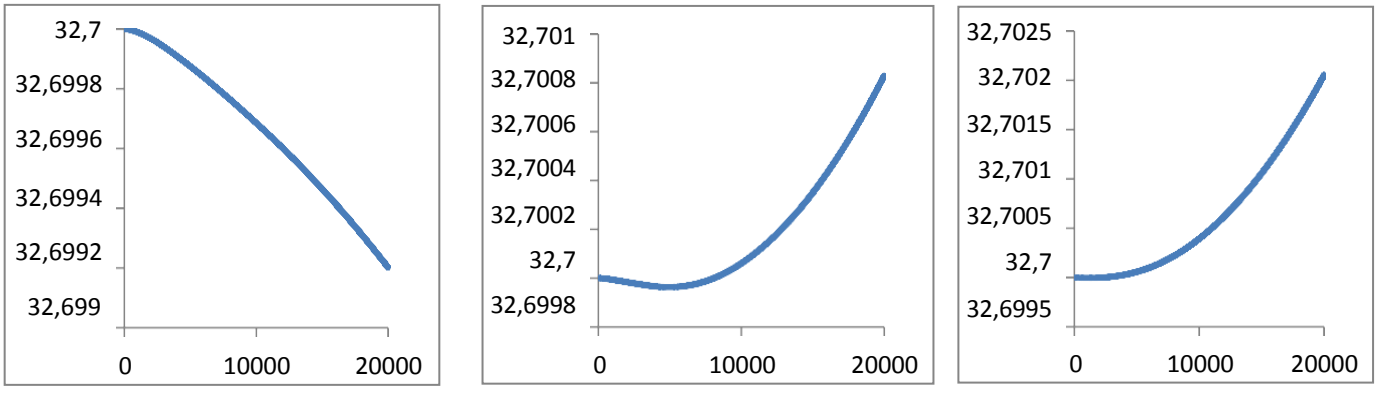


**Figure-7:** Parameter plot for 60% Al. For 60% Al: the appearance is very particular, it starts with a linearity to bend in the opposite direction to other alloys, and this is done around 1350°K.

**Fraction and order parameter: Fraction:** In order to understand this phenomenon of inversion of the behavior observed on the crystalline parameter around 1350°K for the alloy of Ti-60% Al, we were interested in the filling rate of each of these alloys and whatever the temperature the filling rate remains fixed for each percentage of aluminum presented in Table-7.

**Table-7:** Percentage fraction of aluminum.

| Temperature (K) | Formation energy | | |
|---|---|---|---|
| | % Al | | |
| | 40 | 50 | 60 |
| 1300 | 0.4025 | 0.4925 | 0.5815 |
| 1400 | 0.4025 | 0.4925 | 0.5815 |
| 1500 | 0.4025 | 0.4925 | 0.5815 |

In most cases, we find that the filling ratio is close to the percentages of aluminum in the titanium alloy.
For 40% Al: the filling rate is 0.4025, higher than the initial percentage, that is to say a difference of 0.0025, that is to say 0.25%, the structure has more sites to fill, it needs to restructure itself, in other words its instability is considerable;
For 50% Al: the filling rate is 0.4925, lower than the initial percentage, that is to say a difference of 0.0075, or 0.75%;
For 60% Al: the filling rate is 0.5815, lower than the initial percentage, i.e. a difference of 0.0185, or 1.85%.

At this stage we thought that the inversion of the curve of the crystalline parameter is due to the filling rate for the 60%Al titanium alloy because the latter presents a high percentage in filling rate.

**Order parameter:** The filling rate is closely related to the configurations and therefore to the order parameter that we wanted to observe to always understand the behavior of the structure of the titanium alloy at 60% Al in particular. Thus, for the SRO parameter, for a system with an equal number of atom types A and B, a perfectly ordered lattice has a $\sigma=1$, a phase-separated system has a $\sigma=-1$, and a completely random solid solution has a $\sigma=0$. Although it is a simple quantified representation of a potentially complex order, the order parameter is generally interpreted in three values, negative, zero and positive.

For 40% Al: the order parameter is negative close to zero, phase separation structure (towards a random solid solution);
For 50% Al: the order parameter is positive, the system is ordered (towards a random solid solution);
For 60% Al: the order parameter is positive, the system is ordered (towards a random solid solution).

**Table-7**: Order parameter-energy of formation

| Temperature (K) | Order parameter-Formation energy | | | | | |
|---|---|---|---|---|---|---|
| | % Al | | | | | |
| | 40 | Ef | 50 | Ef | 60 | Ef |
| 1300 | -0.004166 | 7.135 | 0.01 | 8.826 | 0.0475 | -0.886 |
| 1400 | -0.004166 | -11.632 | 0.01 | 3.541 | 0.0475 | -13.487 |
| 1500 | -0.004166 | -5.977 | 0.01 | 7.937 | 0.0475 | 1.577 |

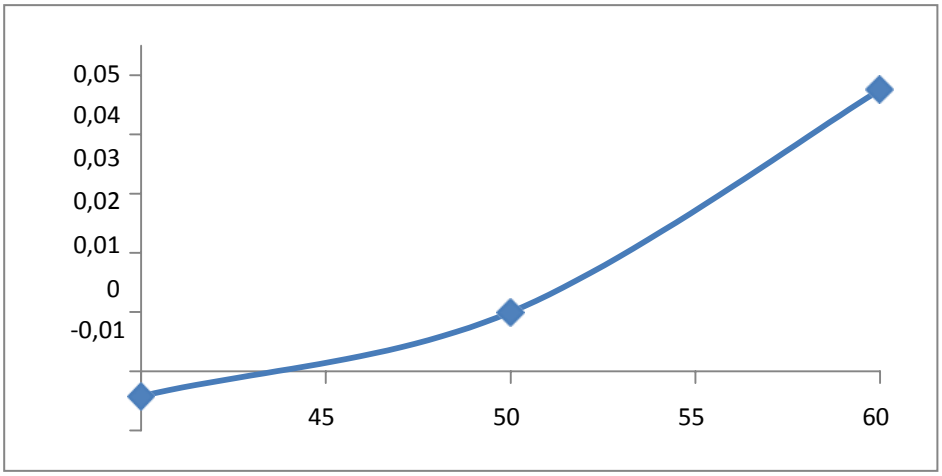


**Figure-8:** Order parameter vs % Al.

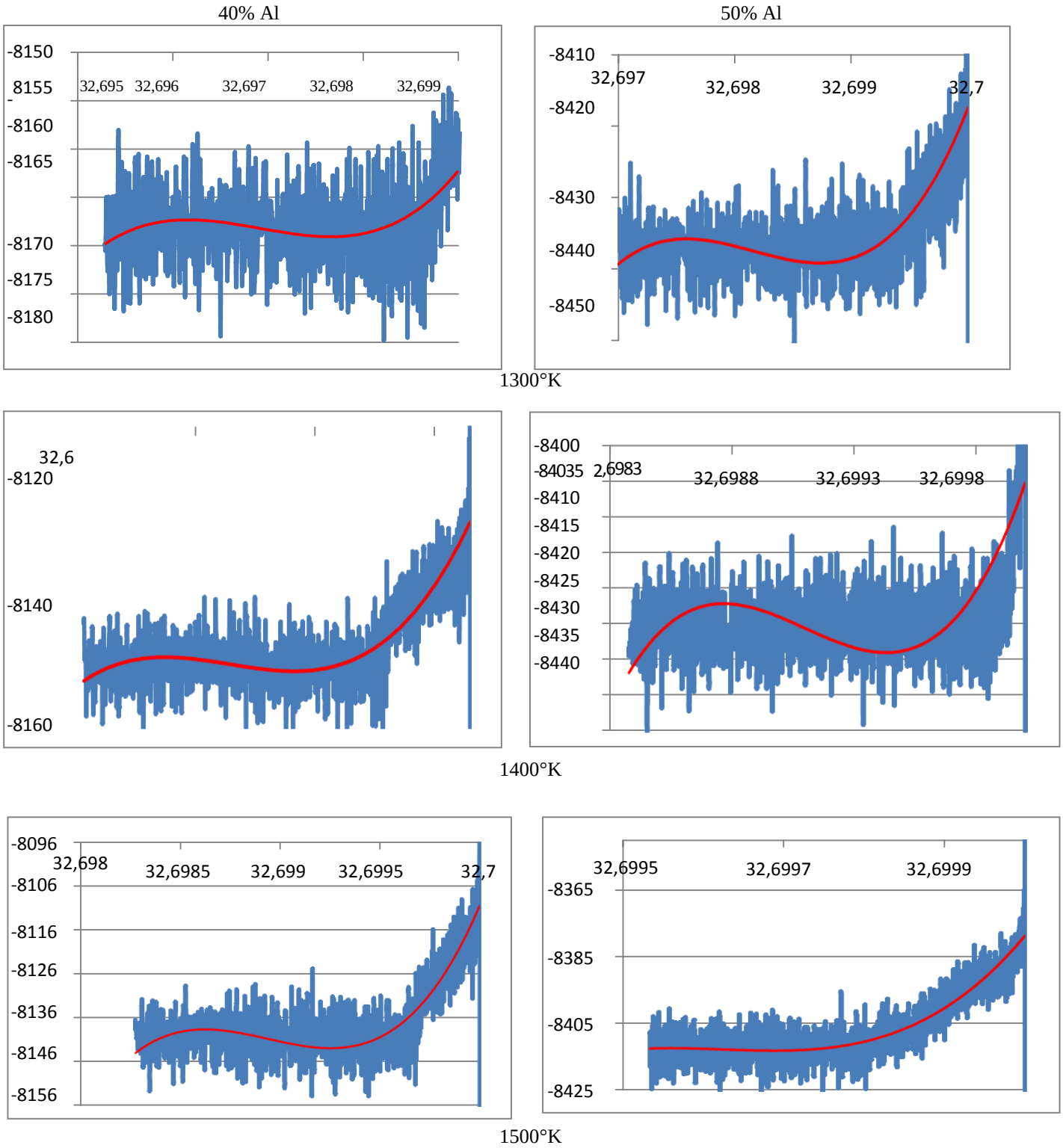


**Figure-9:** Energy: Polynomial trend energy vs crystal parameter for x% Al.

## Conclusion

In this work, we used the MEAM potential of Ti-Al to follow the structural behavior of the B2 type cubic centered phase TiAl alloy in terms of central gap formation energy at 1300, 1400 and 1500 operational temperatures. The results showed us that the Ti-50% Al structure is well stable whatever the operating temperature. Although presenting the same aspect, an opposite

phenomenon is reported for the Ti-60% Al structure whose crystalline parameter increases by 1.85% with temperature; we attributed as cause the filling rate which becomes considerable for Ti-60% Al. Finally, the existence of a gap is not sufficient to conclude the behavior of the structure, different temperatures, but rather the filling rate remains a factor influencing the properties closely related to the structure. An in-depth study on this observed phenomenon remains of scientific interest; however, we will continue this work to understand the influence of the neighbors as well as the state of the structure under different operational temperatures.

## References

**1.** Kothari, K., Radhakrishnan, R., & Wereley, N. M. (2012). Advances in gamma titanium aluminides and their manufacturing techniques. *Progress in Aerospace Sciences*, 55, 1-16.

**2.** Shong, D. S., & Kim, Y. W. (1989). Discontinuous coarsening of high perfection lamellae in titanium aluminides. *Scripta metallurgica*, 23(2), 257-261.

**3.** Antoine PARIS (2015). Study of Phase Transformations in TiAl Alloys with low Silicon Alloying. *Materials*. UNIVERSITÉ DE LORRAINE. French. tel-01394655

**4.** Amélio, S. (2005). Microstructural evolution of a TiAl alloy under dynamic compression and isothermal heat treatment. Doctoral dissertation, Institut National Polytechnique de Lorraine.

**5.** Timothée NSONGO (2001). Computer simulation of order-disorder transformation for TiAl binary system. Ph.D Dissertation, University of Science and Technology Beijing.

**6.** Mohamed BENHAMIDA (2014). Structural, elastic and electronic properties of transition metal nitride alloys. Ph. D. Thesis. University of Setif1-Stif.

**7.** Pascuet, M. I., & Fernández, J. R. (2015). Atomic interaction of the MEAM type for the study of intermetallics in the Al–U alloy. *Journal of Nuclear Materials*, 467, 229-239.

**8.** Pascuet, M. I., & Fernández, J. R. (2015). Atomic interaction of the MEAM type for the study of intermetallics in the Al–U alloy. *Journal of Nuclear Materials*, 467, 229-239.

**9.** Kim, Y. M., Lee, B. J., & Baskes, M. I. (2006). Modified embedded-atom method interatomic potentials for Ti and Zr. *Physical Review B*, 74(1), 014101.

**10.** Mendelev, M. I., & Mishin, Y. (2009). Molecular dynamics study of self-diffusion in bcc Fe. *Physical review B*, 80(14), 144111.

**11.** Mendelev, M. I., & Bokstein, B. S. (2010). Molecular dynamics study of self-diffusion in Zr. *Philosophical Magazine*, 90(5), 637-654.

**12.** Moore, A. P. (2013). Computational Properties of Uranium-Zirconium. Doctoral dissertation, Georgia Institute of Technology.

**13.** Mendelev, M. I., & Bokstein, B. S. (2010). Molecular dynamics study of self-diffusion in Zr. *Philosophical Magazine*, 90(5), 637-654.